International Journal of Heat and Mass Transfer 154 (2020) 119762

Contents lists available at ScienceDirect

International Journal of Heat and Mass Transfer

journal homepage: www.elsevier.com/locate/hmt

Study of phononic thermal transport across nanostructured interfaces using phonon Monte Carlo method

Yu-Chao Hua, Bing-Yang Cao*

Key Laboratory for Thermal Science and Power Engineering of Ministry of Education, Department of Engineering Mechanics, Tsinghua University, Beijing 100084, P R China

ARTICLE INFO

Article history:
Received 17 December 2019
Revised 19 February 2020
Accepted 6 April 2020

Keywords:
Nanostructured interfaces
Interfacial thermal transport
Phonons
Monte Carlo

ABSTRACT

Reducing the phonon-dominated thermal interfacial resistance (TIR) is an effective way to reduce the junction temperature of electronic devices. Several researches have demonstrated that fabricating nanostructures at interface, i.e., constructing nanostructured interface, could significantly enhance the interfacial thermal transport. Here, we conducted a parametrical study on the phononic thermal transport across nanostructured interfaces using phonon Monte Carlo (MC) technique, and analyzed the dependence of effective thermal resistance ratio between the nanostructured and planar interfaces on the various parameters and the heat flux distributions. Our simulations and analyses indicate that the interfacial thermal transport improvement should be attributed to two mechanisms: the change of heat conduction pathways resulted from the interfacial nanostructures and the phonon transmission enhancement induced by the multiple reflection at the interface. The former is predominant when the diffusive transport dominates, while the latter becomes dominant with the enhancement of ballistic transport effect. Additionally, the diffuse scattering of phonons at the interface, which is enhanced with the increasing interface roughness, has a strong negative effect on the improvement of interfacial thermal transport. Due to the combination of those three mechanisms above, the effective thermal resistance ratio decreases to a minimum value and then increases with the increasing contacting area. The present work provides a more in-depth understanding on the interfacial thermal transport in nanostructured interfaces, and can be helpful for the thermal management of electronic devices.

1. Introduction

Effective cooling of electronic devices can greatly improve their performance and reliability, especially for GaN high-electron-mobility transistors (HEMTs) that usually hold a super high-power density [1-5]. In practice, the phonon-dominated thermal interfacial resistance (TIR) plays a crucial role in the heat conduction process within electronic devices, and thus improvement of interfacial thermal transport can effectively reduce the junction temperature [6-9].

Much work has been conducted to understand the phononic interfacial thermal transport [10-16] and to explore applicable methods to enhance it [17-20]. It has been found that various factors, including the phonon density of states (DOS) mismatch [10], chemical bonding [14], interface roughness and structures [17], etc., can greatly influence phonons transport across interface, which offers different approaches to control the phonon-dominated TIR. In a primary stage, most of researches focused on improving the quality of planar interfaces to reduce TIR, such as, adding transition layer between the contacting materials to lower the lattice mismatch [7] and reducing the defects near the interfaces [11]. Nevertheless, some simulations [21-25] revealed that TIR can be greatly reduced via using a non-planar interface, i.e. fabricating nanostructures at an interface. Liang and Sun [21] used the non-equilibrium molecular dynamics (NEMD) technique to study the TIR between Ar solids with different atom masses, and found that a staggered structure at the interface could improve the TIR. Then, the NEMD simulations by Hu et al. [22] also demonstrated that nano-engineering of a GaN-AlN-SiC interface enhanced the phonon transport across the interface. Another MD simulations by Zhou et al. [23] further suggested that such enhancement is proportional to the enlarged contact area due to the nanostructures at the interfaces.

Furthermore, several experiments have been conducted to verify this idea. Lee et al. [26] reported a TDTR (time-domain thermoreflectance)-based experimental demonstration of the thermal transport improvement of nanostructured interfaces between Al and Si, and they explained the mechanism of this enhancement

* Corresponding author.
E-mail address: caoby@tsinghua.edu.cn (B.-Y. Cao).

https://doi.org/10.1016/j.ijheatmasstransfer.2020.119762
0017-9310/

by analogy to the fins used in the traditional heat exchangers. Then, Park et al. [27] identified the similar phenomena for the Al-SiO_2 interfaces in their experiments. They used the Fourier's law-based diffusive equations to simulate the heat conduction within the nanostructured interfaces and attributed such improvement to the change of thermal pathways induced by the interfacial nanostructures. We should note that Fourier's law could be invalid to describe the phonon transport process across interfaces due to ballistic effect [28,29]. Moreover, Cheng et al. [30] experimentally studied the TIR of diamond-Si interfaces, and observed an increased thermal conductivity of diamond owing to the strong grain texturing near the interface. However, the experiments by Hopkins et al. [31] found that growing Ga_xSi_{1-x} quantum dots at the Al-Si interfaces increased the TIR though it should also increase the interfacial contact area, and this phenomenon was explained mainly through the additional diffusive scattering induced by the nanostructured interface. Also, the simulations by Ran et al. [32] found that the effective Kapitza conductance (the inverse of TIR) decreases with the increased interfacial area ratio, because they assumed that the diffuse scattering of phonons is predominant at the interface. Thus, the theory analogue to the fins used in the macroscale heat exchangers may not fully explain the thermal transport across a nanostructured interface, since the influence of diffusive scattering is not involved in it. In fact, the underlying mechanisms of tuning thermal transport across interfaces by nanostructures remain unclear, and it is waiting for further investigations to clarify the factors that can improve or impede the interfacial thermal transport in this case.

In the present paper, a parametrical study on the phononic thermal transport across nanostructured interfaces was conducted using phonon Monte Carlo (MC) simulations to clarify the mechanisms of the thermal transport improvement in this case. Two major mechanisms lead to such thermal transport improvement in a nanostructured interface when compared to a planar case: the change of heat conduction paths resulted from the interfacial nanostructures and the phonon transmission enhancement induced by the multiple-reflection at the interface. By contrast, the diffuse scattering of phonons at the interface can significantly suppress such improvement effect.

2. Problem formulation and simulation details

Fig. 1 shows the schematics of planar and nanostructured interfaces. The contacting materials are labelled by A and B, and they are in contact with the heat sinks of high and low temperatures respectively. We set one interface region, where the nanostructures locate, and two buffer regions in the simulation systems. Their thicknesses are denoted by t_{in} and t_{bu} respectively. Moreover, w_{period} is the width of the simulation period, and w_{in} refers to the width of the periodic unit of interfacial nanostructures. Then we have $w_{in} = w_{period}/n_u$ where n_u is the number of periodic units within one simulation period. The effective thermal resistances of interface regions for both the planar and nanostructured interfaces were calculated and compared to evaluate the influence of nanostructures on the interfacial thermal transport.

In our present work, the phononic thermal transport across interfaces was simulated using phonon MC technique [33]. It is on the basis of the phonon Boltzmann transport equation (BTE) and has been widely applied to investigate the nanoscale thermal transport process involving complicated geometries and heat wave effect. References [34,35] have given the basic principles of this technique. Here, as a parametrical study, Materials A and B in the simulations were not set as a specific kind of material, and the gray-media approximation [36] was adopted for simplicity and clarity. This measure avoids the errors caused by the choice of materials' phonon MFPs and facilitate the analysis, since all the parameters in the simulations can be readily converted into being dimensionless. It is noted that the gray-media approximation could be regarded as solving the phononic thermal transport process in "single phonon mode", and several researchers have pointed out that the influence of phonon dispersion could be incorporated using integral over phonon modes [5,37]. Additionally, the phonon transmissivity was set to be independent on the incident angle in our simulations; therefore, instead of Snell's law that leads to an incident-angle-dependent transmissivity, we assumed that the phonon bundle transmits through the interface ballistically, that is to say, the traveling direction of phonon bundle keeps unchanged. This assumption that corresponds to a limiting case of specular transmission can reflect the influence of specular transmission on thermal transport [16,38].

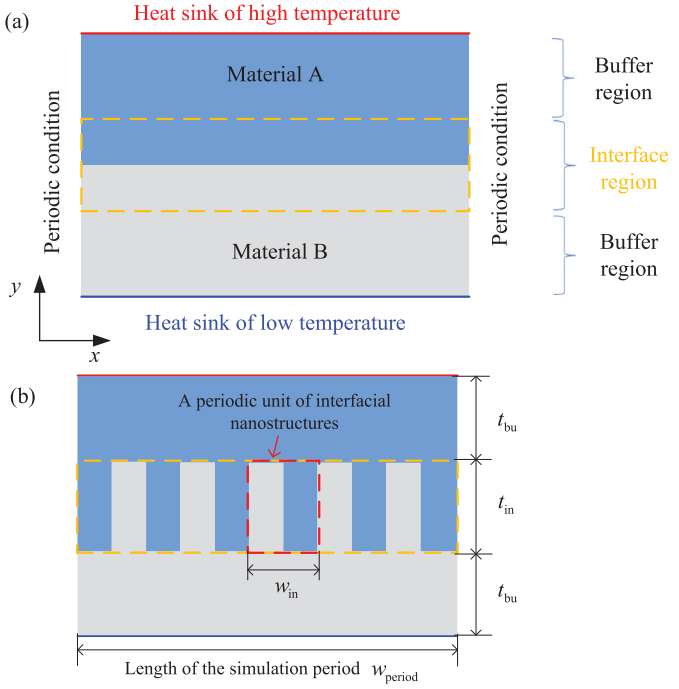

Fig. 1. Schematics of (a) Planar and (b) Nanostructured interfaces.

Here, an effective thermal resistance of interface region, R, is defined as,

$$R = R_{total} - R_{bu,A} - R_{bu,B} = \frac{\Delta T_s}{Q} - \frac{t_{bu}}{\kappa_{0,A}} - \frac{t_{bu}}{\kappa_{0,B}} \quad , \tag{1}$$

where R_{total} is the total thermal resistance of the whole structure that is defined as the ratio between the temperature difference of heat sinks (ΔT_s) and the heat flow (Q), and $R_{bu,\,A(B)}$ is the thermal resistance caused by the buffer region and it is estimated as the ratio between the thickness of buffer region (t_{bu}) and the corresponding intrinsic thermal conductivity ($\kappa_{0,\,A}$ and $\kappa_{0,\,B}$ for Materials A and B respectively). It is noted R avoids the ambiguity in the definition of temperature near the interface [39,40] through using the temperature difference of heat sinks, and it is of clarity and convenience for calculation and evaluating the influence of nanostructured interfaces.

In order to verify our simulation codes, we calculated the effective thermal resistances of interface region for the planar interface and compared them with the model predictions. Based on the phonon BTE, Zeng and Chen [39] obtained a model to calculated the effective thermal conductivity of the superlattice consist of multiple layers. The effective thermal resistance model for the planar interface can be derived from the model by Zeng and Chen,

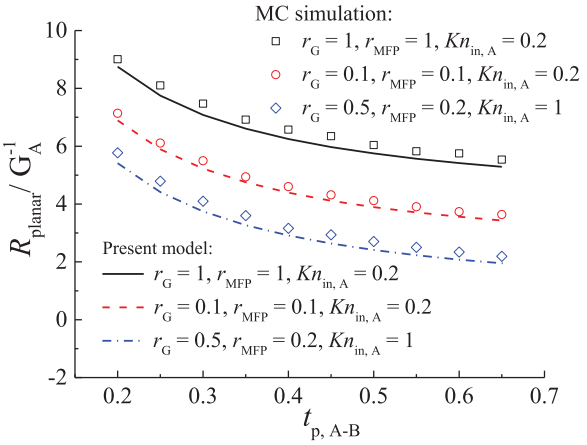

Fig. 2. Effective thermal resistances for the planar interface calculated by the model and MC method.

and it is given by,

$$\frac{R_{planar}}{G_A^{-1}} = \frac{3}{8}\frac{t_{in}}{l_A}\left(1 + \frac{l_A}{l_B}\frac{G_A}{G_B}\right) + \frac{1}{t_{p,A-B}} = \frac{3}{8}\frac{1}{Kn_{in,A}}(1 + r_{MFP}r_G) + \frac{1}{t_{p,A-B}}, \tag{2}$$

in which $t_{p,A-B}$ is the phonon transmissivity from A to B, l_A and l_B are the MFPs of materials A and B respectively, $r_{MFP} = l_A/l_B$ is the MFP ratio, $Kn_{in,A}=l_A/t_{in}$ is the Knudsen number, $G_A = v_{g,A}C_{V,A}/4$ and $G_B = v_{g,B}C_{V,B}/4$ with the group velocity v_g and the heat capacity C_V are the ballistic thermal conductance [40] of materials A and B respectively, and $r_G = G_A/G_B$is the ratio between them. Fig. 2 shows a good agreement between the simulation results and the model predictions for the planar interfaces with different parameter settings. Their maximum deviation is less than 10%, indicating the validity of our codes.

To evaluate the influence of interfacial nanostructures, we calculated the ratio between the effective thermal resistances of interface region for the nanostructured and planar interfaces, and it is given by,

$$r_R = \frac{R_{nano}}{R_{planar}}, \tag{3}$$

where R_{nano} is the effective thermal resistance of interface region for the nanostructured interface. The ratio, r_R, should mainly depend on six independent parameters: the MFP ratio (r_{MFP}), the ratio between the thermal ballistic conductance of contacting materials (r_G), the phonon transmissivity across the interface from A to B ($t_{p,A-B}$), the specularity parameter at the interface (P_s), the number of periodic units within the simulation period (n_u) that is proportional to the enlarged area induced by the interfacial nanostructures, and the Knudsen number ($Kn_{in,A}$) defined by the MFP of material A (l_A) and the thickness of interface region (t_{in}) that reflects the intensity of phonon ballistic transport [15]. The specularity parameter represents the percentage of phonons being specularly reflected or transmitted at the interface. Ziman [41] proposed a model, $P_s = \exp(-4\eta^2\vec{k}^2)$, with the rms roughness η and the phonon wave vector $\vec{k}$, to estimate P_s. This model indicates that the specularity parameter will decrease with the increasing roughness. In fact, the specularity parameter can depend on several parameters, such as roughness, correlation length, and amorphous coating, etc. [42-44] According to Ref. [43], the model by Ziman even cannot accurately predict the specularity parameter in some cases. Although some models [42,44] have been developed to improve the model by Ziman, the specularity parameter has been used as a fitting parameter in many cases, since it is usually difficult to accurately determine all the morphological parameters of boundaries and interfaces in practice. Therefore, in our simulations, the specularity parameter was set to be a specific value rather than calculating from the model by Ziman. Moreover, due to the requirement of energy balance [30,40], the phonon transmissivity from B to A ($t_{p,B-A}$) should be

$$t_{p,B-A} = r_G t_{p,A-B} = \frac{G_A}{G_B} t_{p,A-B}. \tag{4}$$

In addition, the width of simulation period was 10 times of the interface region's thickness ($10t_{in}$), and the thickness of buffer region was the half of the interface region's thickness ($0.5t_{in}$).

3. Results and discussions

The absolute value of one minus the MFP ratio, $|1 - r_{MFP}|$, measures the difference of the ability of phonon transport between the contacting materials. For instance, as $|1\text{-}r_{\_MFP}|$ is equal to 0, the MFP of Material A is the same as that of Material B, and thus the intensity of internal phonon scattering that can impede the phonon transport is identical within those two materials; by contrast, if $|1\text{-}r_{\_MFP}|$ approaches 1, the MFP of Material A is far smaller than that of Material B, indicating that the internal phonon scattering within Material A is much stronger compared to Material B. Fig. 3 shows the dependence of the effective thermal resistance ratio (r_R) on this quantity under different parameter settings. It is found that r_R deceases with the increasing $|1 - r_{MFP}|$, despite the values of other parameters, including r_G, $t_{p,A-B}$, P_s, and n_u. As illustrated in Figs. 4(a) and (b), fabricating interfacial nanostructures between the materials of different phonon MFPs can significantly alter the heat conduction pathways within the interface region [27]. This effect can be characterized by calculating the deviations (d_{qy}) between the y-directional heat flux through the midline of interface region for the nanostructured interface and that for the planar case,

$$d_{qy} = \frac{q_{y\_nano} - q_{y\_planar}}{q_{y\_planar}}, \tag{5}$$

where q_{y_nano} is the y-directional heat flux for the nanostructured interface, while q_{y_planar} is that for the planar case. Fig. 4(c) shows the heat flux deviations between the nanostructured and planar interfaces. We set $P_s = 1$ and $t_{p,A-B} = 1$ to exclude the influence of diffusive phonon scattering and reflection at the interface. A planar interface corresponds to a uniform heat flux through the midline of interface region, and thus the heat flux deviation is equal to zero in this case. As indicated by the heat flux deviations shown in Fig. 4(c), the interfacial nanostructures change the uniform heat flux distribution to the serrated distribution. Moreover, the heat flux deviations between the nanostructured and planar interfaces are enhanced with the increasing disparity of MFPs, $|1 - r_{MFP}|$, which is consistent with the dependence of r_R on $|1 - r_{MFP}|$ shown in Fig. 3. This suggests that the interfacial thermal transport improvement that is enhanced with the increasing $|1 - r_{MFP}|$ can be attributed to the change of heat conduction pathways, i.e., the change of heat flux distributions. This point can be understood through a simple example that is a limiting situation where the phonon transmissivity is equal to 1, the thickness of buffer regions vanishes, and diffusive thermal transport dominates. These three assumptions eliminate the influence of phonon reflection and scattering at the interface, and thus only the change of heat conduction pathways take effects. In this case, the effective thermal resistance for the nanostructured interface is reduced to the total value of thermal resistances in parallel, while that for the planar interface is equal to the total value of thermal resistances in series; thus, r_R

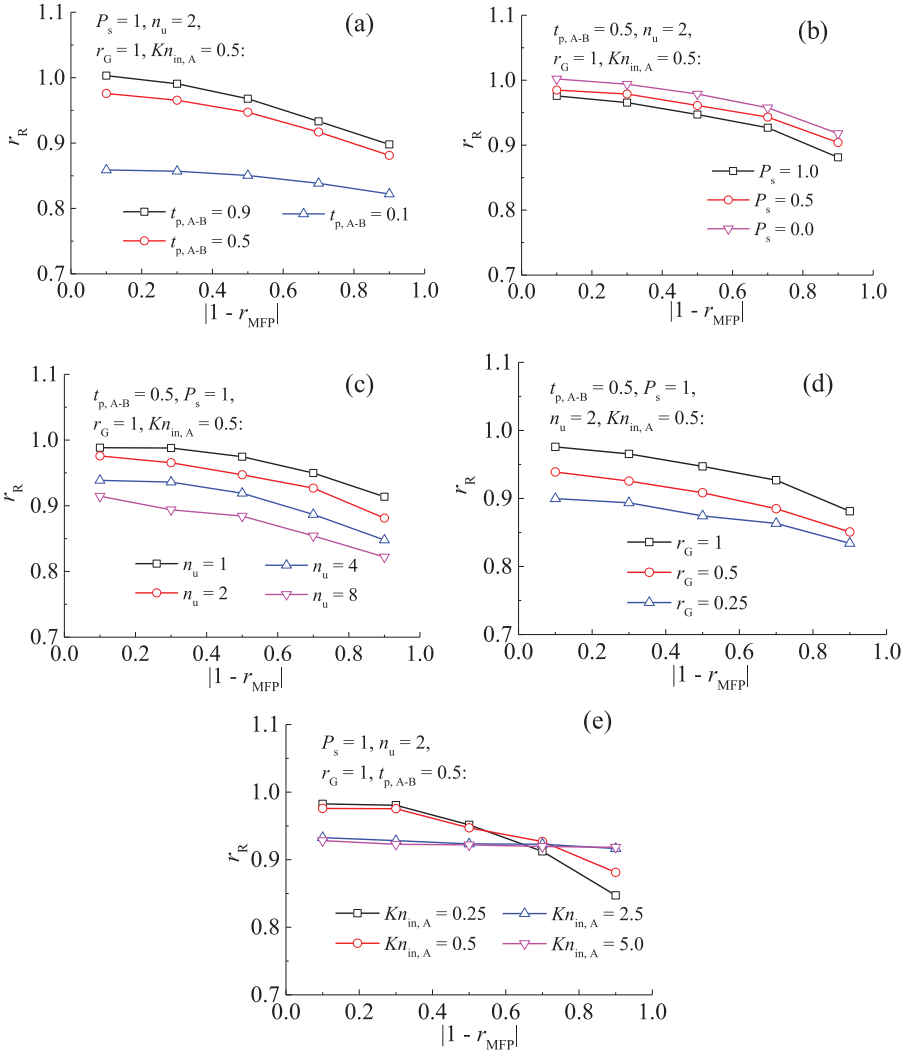

Fig. 3. Effective thermal resistance ratio, r_R, vs. absolute value of one minus the MFP ratio, $|1 - r_{MFP}|$, under different parameter settings: (a) $P_s = 1$, $n_u = 2$, $r_G = 1$, $Kn_{in,A} = 0.5$; (b) $t_{p,A-B} = 0.5$, $n_u = 2$, $r_G = 1$, $Kn_{in,A} = 0.5$; (c) $t_{p,A-B} = 0.5$, $P_s = 1$, $r_G = 1$, $Kn_{in,A} = 0.5$; (d) $t_{p,A-B} = 0.5$, $P_s = 1$, $n_u = 2$, $Kn_{in,A} = 0.5$; (e) $P_s = 1$, $n_u = 2$, $r_G = 1$, $t_{p,A-B} = 0.5$.

is given by,

$$r_{R\_lim} = \frac{\left[\frac{1}{2t_{in}}(\kappa_{0,A} + \kappa_{0,B})\right]^{-1}}{\frac{t_{in}}{2\kappa_{0,A}} + \frac{t_{in}}{2\kappa_{0,B}}} = \frac{4}{2 + \frac{\kappa_{0,A}}{\kappa_{0,B}} + \left(\frac{\kappa_{0,A}}{\kappa_{0,B}}\right)^{-1}} \le 1, \quad (6)$$

which is not greater than 1, indicating that the change of heat conduction pathways alone reduces the effective thermal resistance.

Furthermore, as shown in Fig. 3(e), the dependence of r_R on $|1 - r_{MFP}|$ gradually weakens with the increasing Knudsen number, $Kn_{in,A}$, indicating that the influence from the change of heat conduction pathways degrades with the enhancement of phonon ballistic transport effect, and this point is also confirmed by Fig. 4(c) that shows the heat flux deviations are reduced with the increasing Knudsen number, $Kn_{in,A}$. More importantly, according to Fig. 3(e), there should be other mechanism leading to the thermal transport improvement in this case, since the effective thermal resistance ratio, r_R, is still less than 1 at the large Knudsen numbers.

According to Figs. 5(a) and (b), the number of phonon reflection at the interface increases due to the enlarged interfacial area, and the wall of the nanostructures can provide the additional chance so that those reflected phonons can meet the interface and get another opportunity to be transmitted across the interface. Thus, this multiple reflection effect can reduce the effective thermal resistance ratio. The number of phonon reflection at the interface should increase with the increasing interfacial area (the interfacial area is proportional to the number of periodic units, n_u) and the decreasing phonon transmissivity across the interface ($t_{p,A-B}$). Interestingly, according to Figs. 3(a) and (c), the effective thermal resistance ratio and the number of phonon reflection at the interface have the same trend varying with n_u and $t_{p,A-B}$, when the interfaces are considerably smooth (P_s =1). Then, we calculated the average number of phonon reflection at the interface ($n_{reflection}$), and evaluated the dependence of phonon transmission and effective thermal resistance ratio on this quantity. In Fig. 5(c), the phonon transmission ratio, r_{trans}, is the ratio between the interface region's overall transmissivity for the nanostructured interface and that for the planar case; we set $P_s = 1$ and $|1 - r_{MFP}| = 0$ to exclude the influence of diffuse phonon scattering and heat conduction pathways. The phonon transmission ratio, r_{trans}, is larger than 1 and increases with the increasing $n_{reflection}$, confirming that the multiple reflection at the interface can enhance the overall phonon transmission ratio and reduce the effective thermal resistance ratio. This effect is enhanced with the increasing Knudsen number, and it should be the dominant factor for the interfacial thermal transport improvement in the regime of large Knudsen numbers where the ballistic effect is significant. Moreover, the reduction of

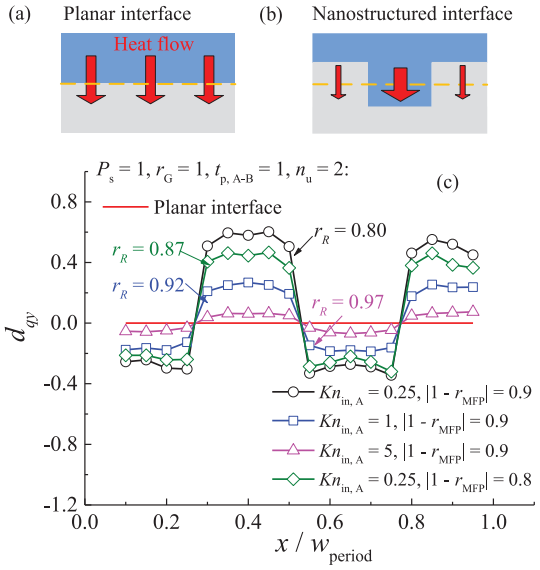

Fig. 4. Schematics of the heat conduction pathways within interface region for (a) planar interface and (b) nanostructured interface; (c) Heat flux deviations between the nanostructured and planar interfaces.

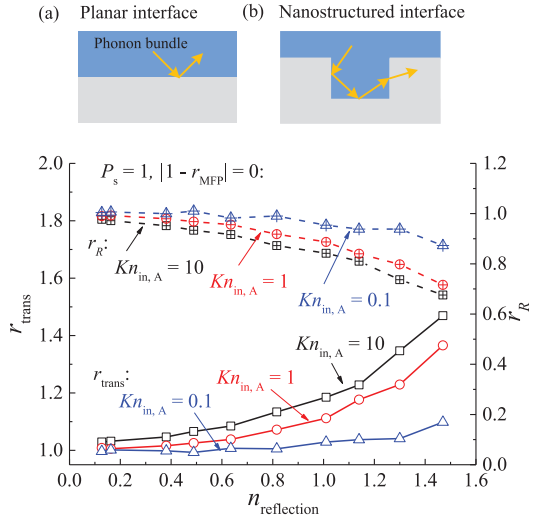

Fig. 5. Schematics of the phonon reflection at interfaces for (a) Planar case and (b) Nanostructured case (where multiple reflection occurs); (c) Phonon transmission ratio (r_{trans}) / effective thermal resistance ratio (r_G) vs. average number of phonon reflection at the interface ($n_{reflection}$).

r_R with the decreasing ballistic thermal conductance ratio, r_G, as shown in Fig. 3(d), could be explained by this effect. Referring to Eq. (4), the phonon transmissivity from B to A, $t_{p,B-A}$, decreases with the decreasing r_G, and thus the reflectivity is enhanced, leading to an increase of $n_{reflection}$. This mechanism also well explains the experimental results by Lee et al. [26] that the Al/Si effective TIR values were not that distinct for the planar and the nanostructured interfaces at low temperatures (< 150 K). With the decreasing temperature, the ballistic transport effect intensifies and the phonon transmissivity across the Al/Si interfaces increases to approximately 1 [45], which significantly suppresses the effects of heat conduction pathways' change and multiple reflection at the interface.

When the interface is not that smooth, the increased interfacial area by nanostructures can intensify the diffuse phonon scattering at the interface that impedes the thermal transport. As an example given in Fig. 6, for a rough interface of $P_s = 0$, r_R increases with the

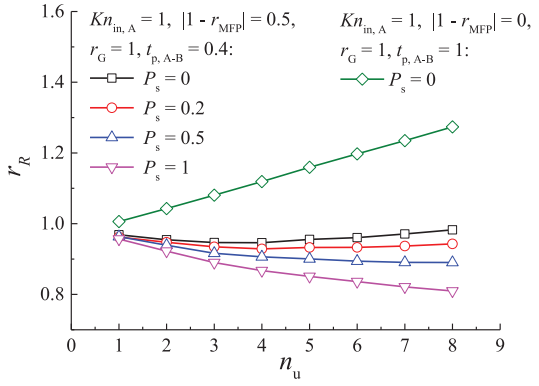

Fig. 6. Effective thermal resistance ratio, r_R, vs. number of periodic units within one simulation period, n_u.

increasing n_u (i.e. the increasing interfacial area), as $|1 - r_{MFP}| = 0$, $r_G = 1$, and $t_{p,A-B} = 1$ that exclude the influence of heat conduction pathways' change and multiple reflection at the interface. Moreover, Fig. 3(b) shows that r_R increases with the decreasing specularity parameter P_s. In general, the specularity parameter decreases with the increasing roughness [37,38]; thus, when the influence of roughness on the phonon transmissivity is not significant, we can conclude that the improvement effect will weaken with the increasing roughness that leads to a stronger diffuse phonon scattering at the interface. This mechanism is supported by the experiments by Hopkins [31]: the nanostructured interface fabricated by growing Ga_xSi_{1-x} quantum dots was rather rough so that the influence of diffuse phonon scattering was predominant and led to an increasing effective TIR. By contrast, when the interface is smooth enough, such as $P_s = 1$, Fig. 6 shows that r_R decreases with the increasing n_u, which confirms the finding by Lee et al. [26] that the effective thermal boundary conductance (the inverse of resistance) can increase with the increasing area enlargement factor of interface (the area ratio between nanostructures and planar) within a certain region, since the area enlargement factor is proportional to the number of periodic units (n_u). In practice, the competition among those three mechanisms above can result in an optimum contacting area that minimizes the effective TIR; as shown in Fig. 6, as $|1 - r_{MFP}| = 0.5$, $t_{p,A-B} = 0.4$, and $P_s < 1$, r_R decreases to a minimum value and then increases with the increasing n_u (i.e. the increasing contacting area).

4. Conclusions

In the present work, the MC technique was used to clarify the mechanisms of thermal transport improvement in the nanostructured interfaces. A uniform heat flux distribution in the case of planar interface is changed to the serrated distribution for the nanostructured interface. Such change of heat conduction pathways can contribute to the improvement of interfacial thermal transport, but its influence decreases with the increasing intensity of ballistic transport effect. Moreover, the wall of the nanostructure can provide the additional chance so that the reflected phonons can meet the interface and get another opportunity to be transmitted across the interface, and such phonon transmission enhancement induced by the multiple reflection becomes predominant when the ballistic transport dominates. By contrast, when the interface is not that smooth, the increased interfacial area by nanostructures also intensifies the diffuse phonon scattering at the interface, which significantly suppresses the interfacial thermal transport improvement. Importantly, due to the competition among those three mechanisms above, the effective thermal resistance ratio decreases to a minimum value and then increases with the increasing contacting

area. Therefore, in practice, there should exist an optimum contacting area that minimizes the effective TIR for a specific type of nanostructured interface.

Declaration of competing interests

The authors declare that they have no known competing financial interests or personal relationships that could have appeared to influence the work reported in this paper.

CRediT authorship contribution statement

Yu-Chao Hua: Conceptualization, Methodology, Software, Validation, Formal analysis, Investigation, Data curation, Visualization, Writing - original draft, Writing - review & editing. **Bing-Yang Cao:** Supervision, Project administration, Funding acquisition.

Acknowledgments

This work is financially supported by National Natural Science Foundation of China (No. 51825601, 51906121, 51676108), the Initiative Postdocs Supporting Program of China Postdoctoral Science Foundation(No. BX20180155), Project funded by China Postdoctoral Science Foundation (No. 2018M641348), Science Fund for Creative Research Group (No. 51321002), the Tsinghua National Laboratory for Information Science and Technology of China (TNList).

Supplementary materials

Supplementary material associated with this article can be found, in the online version, at doi:10.1016/j.ijheatmasstransfer.2020.119762.

References

[1] A.L. Moore, L. Shi, Emerging challenges and materials for thermal management of electronics, Mater. Today 17 (2014) 163–174.
[2] H. Kim, V. Tilak, B.M. Green, et al., Reliability evaluation of high power AlGaN/GaN HEMTs on SiC substrate, Phys. Status Solidi. A 188 (2001) 203–206.
[3] Y. Won, J. Cho, A. Damena, et al., Fundamental cooling limits for high power density gallium nitride electronics, IEEE Trans. Compon. Packag. Manuf. Technol. 5 (2015) 737–744.
[4] Z. Liao, C. Guo, M. Ju, et al., Thermal evaluation of gan-based HEMTs with various layer sizes and structural parameters using finite-element thermal simulation, Microelectr. Reliab. 74 (2017) 52–57.
[5] Y.-C. Hua, H.-L. Li, B.-Y. Cao, Thermal spreading resistance in ballistic-diffusive regime for GaN HEMTs, IEEE Trans. Electr. Devices 66 (2019) 3296–3301.
[6] H.C. Nochetto, N.R. Jankowski, A. Cohen, The impact of GaN/Substrate thermal boundary resistance on a HEMT device, in: Proceedings of the ASME 2011 International Mechanical Engineering Congress & Exposition, 2011.
[7] J. Cho, E. Bozorg-Grayeli, D.H. Altman, et al., Low thermal resistances at GaN-SiC interfaces for HEMT technology, IEEE Electr. Devices Lett. 33 (2012) 378–380.
[8] J.W. Cho, et al., Improved thermal interfaces of GaN-diamond composite substrates for HEMT applications, IEEE Trans. Compon. Packag. Manuf. Technol. 3 (2013) 79–85.
[9] K.A. Filippov, A.A. Balandin, The effect of the thermal boundary resistance on self-heating of ALGaN/GaN HFETs, MRS Internet J. Nitride Semicond. Res. 8 (2003) 4 MRS Internet J. Nitride Semicond. Res..
[10] E.T. Swartz, R.O. Pohl, Thermal boundary resistance, Rev. Mod. Phys. 61 (1989) 605–668.
[11] R.M. Costescu, M.A. Wall, D.G. Cahill, Thermal conductance of epitaxial interfaces, Phys. Rev. B 67 (2003) 054302.
[12] P.E. Hopkins, Thermal transport across solid interfaces with nanoscale imperfections: effects of roughness, disorder, dislocations, and bonding on thermal boundary conductance, ISRN Mech. Eng. 2013 (2013) 1–19.
[13] R. Cheaito, Thermal boundary conductance accumulation and interfacial phonon transmission: measurements and theory, Phys. Rev. B 91 (2015) 035432.
[14] M.D. Losego, M.E. Grady, N.R. Sottos, et al., Effects of chemical bonding on heat transport across interfaces, Nat. Mater. 11 (2012) 502–506.
[15] Y.-C. Hua, B.-Y. Cao, Slip boundary conditions in ballistic–diffusive heat transport in nanostructures, Nanosc. Microsc. Therm. 21 (2017) 159–176.
[16] Y.-C. Hua, B.-Y. Cao, Interface-based two-way tuning of the in-plane thermal transport in nanofilms, J. Appl. Phys. 123 (2018) 114304.
[17] P.E. Hopkins, L.M. Phinney, J.R. Serrano, T.E. Beechem, Effects of surface roughness and oxide layer on the thermal boundary conductance at aluminum/silicon interfaces, Phys. Rev. B 82 (2010) 085307.
[18] P.M. Norris, N.Q. Le, C.H. Baker, Tuning phonon transport: from interfaces to nanostructures, J. Heat Transf. 135 (2013) 061604.
[19] X. Wei, T. Zhang, T. Luo, Molecular fin effect from heterogeneous self-assembled monolayer enhances thermal conductance across hard-soft interfaces, ACS Appl. Mater. Interfaces 9 (2017) 33740–33748.
[20] R. Rastgarkafshgarkolaei, J. Zhang, C.A. Polanco, N.Q. Le, A.W. Ghosh, P.M. Norris, Maximization of thermal conductance at interfaces via exponentially mass-graded interlayers, Nanoscale 11 (2019) 6254–6262.
[21] X.-G. Liang, L. Sun, Interface structure influence on thermal resistance across double-layered nanofilms, Microscale Thermophys. Eng. 9 (2005) 295–304.
[22] M. Hu, X. Zhang, D. Poulikakos, C.P. Grigoropoulos, Large “near junction” thermal resistance reduction in electronics by interface nanoengineering, Int. J. Heat Mass Transf. 54 (2011) 5183–5191.
[23] X.W. Zhou, R.E. Jones, C.J. Kimmer, J.C. Duda, P.E. Hopkins, Relationship of thermal boundary conductance to structure from an analytical model plus molecular dynamics simulations, Phys. Rev. B 87 (2013) 094303.
[24] R.K. Hafez Raeisi Fard, Joel Plawsky, Theodorian Borca-Tasciuc, Reducing thermal interface impedance using surface engineering, 14th IEEE ITHERM Conference, 2014.
[25] E. Lee, T. Zhang, M. Hu, T. Luo, Thermal boundary conductance enhancement using experimentally achievable nanostructured interfaces - analytical study combined with molecular dynamics simulation, Phys. Chem. Chem. Phys. 18 (2016) 16794–16801.
[26] E. Lee, T. Zhang, T. Yoo, Z. Guo, T. Luo, Nanostructures significantly enhance thermal transport across solid interfaces, ACS Appl. Mater. Interfaces 8 (2016) 35505–35512.
[27] W. Park, A. Sood, J. Park, M. Asheghi, R. Sinclair, K.E. Goodson, Enhanced thermal conduction through nanostructured interfaces, Nanosc. Microsc. Therm. 21 (2017) 134–144.
[28] Y. Hu, L. Zeng, A.J. Minnich, M.S. Dresselhaus, G. Chen, Spectral mapping of thermal conductivity through nanoscale ballistic transport, Nat. Nanotechnol. 10 (2015) 701–706.
[29] Y.-C. Hua, B.-Y. Cao, Ballistic-diffusive heat conduction in multiply-constrained nanostructures, Int. J. Therm. Sci. 101 (2016) 126–132.
[30] Z. Cheng, et al., Tunable thermal energy transport across diamond membranes and diamond-Si interfaces by nanoscale graphoepitaxy, ACS Appl. Mater. Interfaces 11 (2019) 18517–18527.
[31] P.E. Hopkins, J.C. Duda, C.W. Petz, J.A. Floro, Controlling thermal conductance through quantum dot roughening at interfaces, Phys. Rev. B 84 (2011) 035438.
[32] X. Ran, Y. Guo, M. Wang, Interfacial phonon transport with frequency-dependent transmissivity by Monte Carlo simulation, Int. J. Heat Mass Transf. 123 (2018) 616–628.
[33] H. Bao, J. Chen, X. Gu, B. Cao, A review of simulation methods in micro/nanoscale heat conduction, ES Energy Environ. (2018), doi:10.30919/esee8c149.
[34] Y.-C. Hua, B.-Y. Cao, Phonon ballistic-diffusive heat conduction in silicon nanofilms by Monte Carlo simulations, Int. J. Heat Mass Transf. 78 (2014) 755–759.
[35] Y.-C. Hua, B.-Y. Cao, An efficient two-step Monte Carlo method for heat conduction in nanostructures, J. Comput. Phys. 342 (2017) 253–266.
[36] A. Majumdar, Microscale heat conduction in dielectric thin films, J. Heat Transfer. 115 (1993) 7–16.
[37] M. Ohnishi, J. Shiomi, Towards ultimate impedance of phonon transport by nanostructure interface, APL Mater. 7 (2019) 013102.
[38] D. Li, A.J.H. McGaughey, Phonon dynamics at surfaces and interfaces and its implications in energy transport in nanostructured materials—an opinion paper, Nanosc. Microsc. Therm. 19 (2015) 166–182.
[39] G. Chen, T. Zeng, Nonequilibrium phonon and electron transport in heterostructures and superlattices, Microsc. Thermophys. Eng. 5 (2001) 71–88.
[40] G. Chen, Thermal conductivity and ballistic-phonon transport in the cross–plane direction of superlattices, Phys. Rev. B 57 (1998) 14958–14973.
[41] J.M. Ziman, Electrons and Phonons: The Theory of Transport Phenomena in Solids, OUP Oxford, 2001.
[42] A.A. Maznev, Boundary scattering of phonons: specularity of a randomly rough surface in the small-perturbation limit, Phys. Rev. B 91 (2015) 134306.
[43] C. Shao, Q. Rong, M. Hu, H. Bao, Probing phonon–surface interaction by wave–packet simulation: effect of roughness and morphology, J. Appl. Phys. 122 (2017) 155104.
[44] P. Jiang, L. Lindsay, X. Huang, Y.K. Koh, Interfacial phonon scattering and transmission loss in >1μm thick silicon-on-insulator thin films, Phys. Rev. B 97 (2018) 195308.
[45] C. Hua, X. Chen, N.K. Ravichandran, and A.J. Minnich, Fresnel transmission coefficients for thermal phonons at solid interfaces, arXiv:1509.07806, 2015.